Journal of Alloys and Compounds, 207/208 (1994) 349–354
JALCOM 3086

Synthesis and properties of aluminum-based metallic glasses containing rare earths

Y. He[a], G.J. Shiflet[b] and S.J. Poon[a]
[a]*Department of Physics,* [b]*Department of Materials Science and Engineering, University of Virginia, Charlottesville, VA 22901 (USA)*

Abstract

A new family of metallic glasses containing up to 92 at.% of aluminum has been synthesized in Al–TM–RE (where TM = transition metals, RE = yttrium and rare earths) alloy systems using a melt-spinning technique. The atomic structure, mechanical properties, thermal and mechanical stability of these metallic glasses have been studied. Structural studies by pulsed neutron and X-ray scattering indicate a strong interaction between Al and transition metal atoms, which may be responsible for the high glass formability of these alloys. Furthermore, the results show that the rare earth atoms play an important role in stabilizing the amorphous structure in these alloys. Mechanical testing reveals that these Al-based metallic glasses have high tensile strengths up to ~1300 MPa, approximately three times that of conventional aluminum alloys. Experimental results show that the tensile strength of these glassy alloys approaches the theoretical value. Thermal stability studies suggest that the formation of these Al-based metallic glasses is rather unusual, since they can readily be formed in the regions where a eutectic region is absent. It was found that the glass formability of these alloys is greatly enhanced by replacing a few percent of rare earth with a second transition metal element. As a result, sub-millimeter thick amorphous ribbons can be obtained at slow cooling rates. It may be possible to obtain bulk amorphous alloys by further optimizing the composition. High tensile strengths combined with good glass formability make these Al glasses ideal candidates for high-strength low-density materials.

1. Introduction

Amorphous alloys or metallic glasses are metallic alloys in which the long-range atomic order is absent. Since the initial synthesis of metallic glass in Au_4Si alloy by splat quenching method in 1960 [1], great effort has been devoted to understand the formation, atomic structures, mechanical and magnetic properties of metallic glasses because of their potential technological applications [2]. For example, amorphous alloys generally have high mechanical strength and good corrosion resistance behavior resulting from their amorphous structure.

Metal melts usually crystallize when cooled below their melting points. However, if the cooling rate is fast enough ($10^6 \sim 10^{12}$ K s^{-1}) by heat removal to a sink, so that the nucleation and crystallization processes are suppressed kinetically, then the supercooled metal liquid will solidify at a temperature T_g lower than the melting temperature T_m into a liquid-like amorphous state, forming an amorphous alloy or metallic glass. This temperature T_g is called the glass transition temperature, where liquid-to-glass transition occurs. Glass formation is therefore a matter of bypassing crystallization. In principle, all materials may be prepared as amorphous solids providing that the cooling rate is high enough and the final temperature is lower than T_g so that spontaneous crystallization will not occur. The critical cooling rate for glass formation varies from system to system. For silicate glasses and many organic polymers, this can be as low as 10^{-2} K s^{-1} due to their covalent bonding nature. For metals, this critical cooling rate may be as high as 10^{12} K s^{-1} because of the non-directional nature of the metallic bond.

Amorphous alloys may be prepared using vapor deposition, chemical deposition and rapid liquid quenching methods. One of the most frequently used methods used to obtain amorphous alloys is the single-roller melt spinning. In this technique, an alloy ingot is first prepared by arc-melting nominal amounts of high purity elements together. Then the ingot is cut into small pieces and induction melted in a quartz tube which has a small nozzle at one end. The metallic liquid is injected through that nozzle onto a rotating copper wheel and solidifies rapidly.

2. Synthesis of aluminum-based metallic glasses

For the past three decades, many metallic alloys have been amorphized using rapid solidification techniques

SSDI 0925-8388(93)03086-X

[3], but very few of them are based on aluminum [4]. Researchers have made great effort to amorphize Al-based alloys by melt quenching, not only to satisfy their scientific curiosity, but also for technological reasons, since aluminum alloys are very light and have a wide range of applications. Previously, only small fractions of glassy phase have been observed in various Al-binary alloys on rapid solidification, notably in Al–X (X = Si, Ge, Cu, Ni, Cr and Pd) alloys. The first successful production of a homogeneous Al-based amorphous phase was achieved in Al–(Fe,Co)–B [5] and Al–Fe–(Si, Ge) ternary alloys [6]. However, these amorphous alloys are extremely brittle, and their tensile strength is as low as about 50–150 MPa, therefore, they have no practical applications.

A new family of metallic glasses that contain up to 92 at.% of aluminum were discovered independently by two groups a few years ago [7,8]. These metallic glasses were found to have very good mechanical properties, with tensile strength as high as 1280 MPa in some systems [9,10]. Thus, they are good candidates for high-strength low-density engineering materials.

In our group, these Al-rich metallic glasses were discovered during the search for aluminum-rich quasicrystals in the $Al_{20}Cr_2Ce$-type alloys ($Al_{18}Cr_2Mg_3$ structure, 184 atoms per unit cell) [11]. In this process, an Al-rich metallic glass of composition $Al_{20}Fe_2Ce$ was obtained, which was produced in continuous ribbons by single-roller melt spinning. This has led to the synthesis of many metallic glasses containing up to more than 90 at.% aluminum. Many of these metallic glasses were found to be flexible with good local ductility, and the amorphous ribbons can be bent 180° without fracture. It was also found that the amorphous phase formation range in this new family of metallic glasses can be as wide as 30 at.% or more. The experimental details can be found elsewhere [7,10].

Systematic investigations revealed that Al-rich metallic glasses can be formed in Al–TM–RE ternary alloy systems, where TM = Fe, Co and Ni, RE = yttrium and rare earth metals [7,8,12]. In addition, metallic glass formation in Al–Rh–RE [7] and Al–Ce–M (M = Nb, TM or Cu, Cr, V, Mn) [12] were also reported. This new group of amorphous alloys based on Al generally contain some transition metals and rare earths or Y, and no single amorphous phase can be formed in binary Al–TM systems by melt quenching. On the other hand, adding as low as 1 at.% of rare earths or Y to Al–TM alloys can greatly enhance the glass-forming ability [13]. For example, replacing 1 at.% of Ni by Gd or Hf in $Al_{85}Ni_{15}$ (which forms fcc-Al and Al_3Ni crystalline phases after melt-spinning) promotes the formation of amorphous and nanocrystalline Al phases [13]. In fact, amorphous phase formation has been reported in Al–RE binary systems [14,15], although they are more difficult to form and the mechanical properties are not as good as Al–TM–RE ternary amorphous alloys.

3. Mechanical properties

3.1. Tensile strength, Young's modulus, microhardness and density

The mechanical properties of Al-based metallic glasses, which include the tensile strength σ_f, Young's modulus E, microhardness (Vicker's hardness) H_v and the density ρ were measured. Many of these glasses were found to have tensile strengths over 800 MPa, greatly exceeding that of conventional aluminum alloys. The Young's moduli were close or greater that of pure Al, depending on the composition. Microhardness values ranging from 250 to 500 DPN (diamond pyramid number, 1 DPN = 1 kg mm^{-2} = 9.8 MPa) were reported. These mechanical properties are given in Table 1 for a few selected compositions. It should be noted that, in general, an increase in microhardness values is observed with increasing load, and this effect occurs with a wide range of materials, from as soft as copper to fully hardened steel. Thus, it is necessary to specify the load used in the measurements.

From Table 1 it is clear that these amorphous alloys exhibit high tensile strengths and low densities. The specific strength σ_s, which is defined as the ratio of σ_f and ρ, is twice that of conventional Al-alloys which have σ_f ranging from 150 MPa to 500 MPa and densities around 3 g mm^{-3}. For some quaternary amorphous alloys, the fracture tensile strength σ_f approaches the theoretical limit, $E/50$. It has been found that by replacing a few percent of Al with a second transition

TABLE 1. Mechanical properties of some Al-based metallic glasses which contain yttrium or rare earths

Composition	σ_f (MPa)	E (GPa)	H_v (DPN)	ρ (g cm^{-3})	Ref.
$Al_{90}Fe_5Ce_5$	940	66	250[a,c]	3.21[c]	7
$Al_{87}Ni_{8.7}Y_{4.3}$	880	50	270[a,c]	3.15[c]	7
$Al_{87}Fe_{8.7}Gd_{4.3}$	840	53	310[a,c]	3.37[c]	7
$Al_{87}Co_{8.7}Ce_{4.3}$	790	63	280[a,c]	3.27[c]	7
$Al_{87}Rh_{8.7}Ce_{4.3}$	730	63	–	3.65[c]	7
$Al_{87}Ni_5Y_8$	1140	71.2	300[b]	3.10[c]	8
$Al_{88}Ni_{10}Y_2$	920	71	340[b]	–	8
$Al_{85}Ni_5Y_{10}$	920	62.8	380[b]	–	8
$Al_{85}Ni_{7.5}Y_{7.5}$	730	84.2	360[b]	–	8
$Al_{85}Ni_5Y_8Co_2$	1250	74	350[b]	–	9
$Al_{85}Ni_5Y_7Co_3$	1140	71.2	340[b]	–	9
$Al_{85}Ni_5Fe_2Gd_8$	1210	75.3	–	3.71	10
$Al_{87}Ni_6FeGd_6$	1140	67.1	–	3.47	10
$Al_{85}Ni_6Fe_3Gd_6$	1280	72.7	–	3.51	10

[a]Load = 20 g. [b]Load = 100 g. [c]He, Poon and Shiflet, University of Virginia, unpublished results.

metal, the tensile strengths of these amorphous alloys can be further improved. The high strength observed in Al-based metallic glasses is related to the amorphous structure and chemical bonding nature of the alloys.

3.2. Ductility

Al-based metallic glasses, like most liquid-quenched amorphous ribbons, can be bent 180° without fracture. Thus, bending tests indicate that many Al-rich metallic glasses with high strength are very ductile, but the tensile plastic strain in an amorphous alloy is very small (<1%) because an amorphous specimen undergoes highly localized shear deformation. On the other hand, a 10% plastic strain (or thickness reduction) was observed when rolling an $Al_{90}Fe_5Gd_5$ glass ribbon once at room temperature [16]. It is generally accepted that a metallic glass can be termed as "ductile" if the fracture occurs as a result of, at least locally, large plastic strain, in contrast with oxide glasses. Indeed, evidence of large local plastic strain is observed when examining the fracture surfaces of Al-based metallic glasses using a scanning electron microscope [17]. Figure 1 is a scanning electron microscopy (SEM) micrograph of a fracture surface of an $Al_{90}Fe_5Gd_5$ metallic glass after tensile testing. This micrograph consists of two distinct regions: a smooth region and a region with vein or river pattern. The smooth region is due to the slip along the shear plane under tension, while the characteristic vein or river pattern is the result of an instability that occurs during the propagation of the cracks inside the metallic glasses [18]. The vein structure consists of protrusions on the fracture surfaces. These markings can be taken as evidence of local necking. The observed fracture features are fairly typical of metallic glass materials. Thus, one can infer that Al-based amorphous alloys have good ductility comparable to conventional ductile amorphous alloys (such as Fe-based metallic glasses or Pd–Cu–Si).

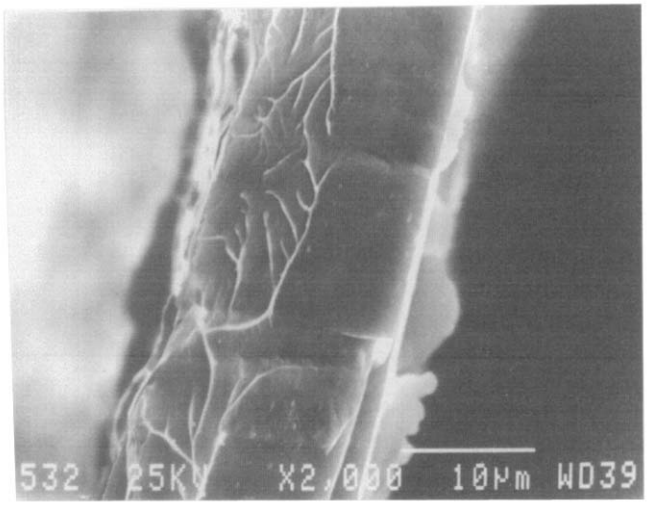

Fig. 1. SEM micrograph of a typical fracture surface of an Al-based metallic glass. This surface contains two distinct features: a smooth area which is due to the slip along the plane of the maximum resolved shear stress, and the vein pattern.

4. Atomic structure

The structural nature of Al-based metallic glasses was studied using conventional X-ray diffraction, transmission electron microscopy (TEM), high-resolution electron microscopy and differential scanning calorimetry (DSC) [19]. It has been a subject of intensive debate whether a material exhibiting a broad diffuse X-ray diffraction pattern has a truly amorphous structure or it consists of randomly oriented microcrystallites [20]. Modern high-resolution electron microscope with a resolution better than 2 Å enables the direct identification of possible microcrystallinity in the sample. Figure 2 is a HREM image of a rapidly solidified $Al_{90}Fe_5Gd_5$ ribbon. This micrograph indicates no crystalline phase on the nanometer scale.

DSC can be used to study the isothermal crystallization kinetics of Al-based metallic glasses. This study allows differentiation between the amorphous and microcrystalline structures, as discussed in [20]. Our experimental results showed that the isothermal DSC signal characterizing the crystallization of Al-based metallic glasses can well be described by nucleation and growth process [10,19], which verifies the amorphous nature of these Al-based metallic glasses.

The atomic structure and short range ordering of liquid-quenched amorphous $Al_{90}Fe_xCe_{10-x}$ ($x=5$, 7) were studied by intense X-ray and pulsed neutron scattering [21,22]. In these studies, the atomic pair-

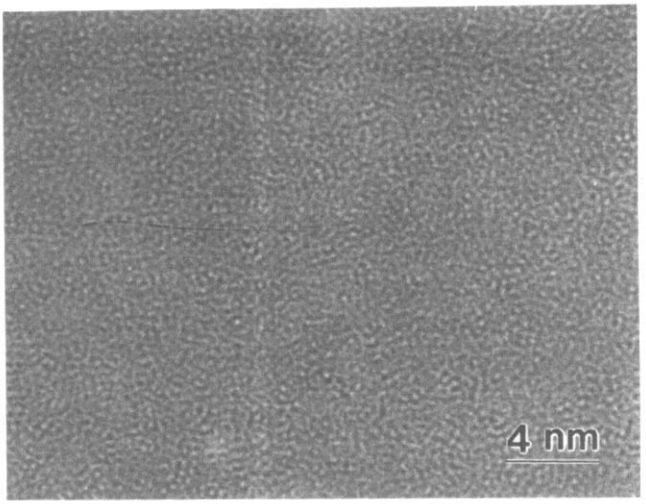

Fig. 2. HREM image of a melt-spun $Al_{90}Fe_5Gd_5$ sample [19]. No crystalline phase can be found. This image confirms the amorphous nature of Al-based metallic glasses.

density function (PDF) $\rho(r)$ can be determined by pulsed neutron and X-ray scattering experiments, which in turn will yield information about nearest neighbor distances and coordination numbers in the structure. A recent review of structural studies using PDF analysis was presented by Egami [23].

The atomic pair-density function determined from neutron and X-ray scattering reveals that a significant portion of Al–Fe bonds is anomalously short in amorphous Al–Fe–Ce alloys. The nearest Al–Fe bond length is only 2.49 Å, 0.2 Å less than the sum of the atomic radii of Al (1.43 Å) and Fe (1.26 Å). This suggests a strong interaction between Al and Fe atoms. Such interaction modifies the structure of the glass, leading to chemical and topological short-range ordering, which contributes to the easy glass formation of these Al-alloys [21,22]. Furthermore, PDF analysis revealed that the local structure of Al–Ce might be described well by the dense random packing model, provided that the Ce–Ce potential is repulsive. The randomly distributed rare earth atoms further stabilizes the amorphous structure of Al–TM–RE metallic glasses.

5. Structural stability

5.1. Thermal stability

Amorphous alloys are not stable, they transform to crystalline phases upon heating. After full crystallization, all the unique properties of a metallic glass are lost. Therefore, it is important to know the thermal stability of a metallic glass before using it in application. The thermal stability of an amorphous alloy can be correlated to its crystallization temperature T_x or glass transition temperature T_g, and the activation energy of crystallization. Usually, the higher the T_g or T_x, the more stable the glasses.

The most useful experimental technique for quickly examining thermally induced structural changes in metallic glasses is differential scanning calorimetry (DSC). In a continuously heating experiment, the DSC trace corresponding to crystallization is one or a series of exothermic peak(s), the area of each peak corresponds to the change of enthalpy ΔH_x during structural transformation. The onset temperature of the first exothermic peak can be taken as the crystallization temperature. The glass transition in metallic glasses, on the other hand, is a kinetic phenomena observed in non-isothermal DSC experiments. When the temperature is approaching T_g, the specific heat of a glass C_p increases to a maximum, then levels off to a constant value; thus a small endothermic signal will appear in DSC scans near the glass transition [24], and T_g is taken as the onset temperature of this endothermic signal. For those metallic glasses where T_x precedes T_g, this endothermic signal cannot be observed since crystallization takes place first.

In the DSC experiments studying the thermal stability of Al-base metallic glasses, two different cases can be distinguished: (1) for some compositions, the first exothermic peak corresponds to the precipitation of pure Al, which occurs at relatively lower temperature near 170 °C to 230 °C, this peak is usually broad and shallow; (2) for other compositions, the primary crystallization of pure Al cannot be detected in a DSC scan, the first exothermic peak occurs at higher temperature (250–350 °C) and is quite sharp. Figure 3 shows these two types of DSC traces. The glass transition temperatures and the first crystallization temperatures of several Al-based metallic glasses are listed in Table 2. Isothermal DSC experiments have been used to estimate the activation energy of crystallization, which is a measure of kinetic resistance to crystallization. The results showed that the activation energy of crystallization of these Al-based amorphous alloys is 3–4 eV, suggesting that they are quite stable at room temperature [10,19].

Annealing experiments have also been performed to ascertain the thermal stability of these metallic glasses. For example, after annealing amorphous $Al_{85}Ni_5Fe_2Gd_8$ and $Al_{85}Ni_6Fe_3Gd_6$ alloys at 200 °C for 15 h, both samples were found to remain in amorphous states with no trace of any crystalline phase in the X-ray diffraction

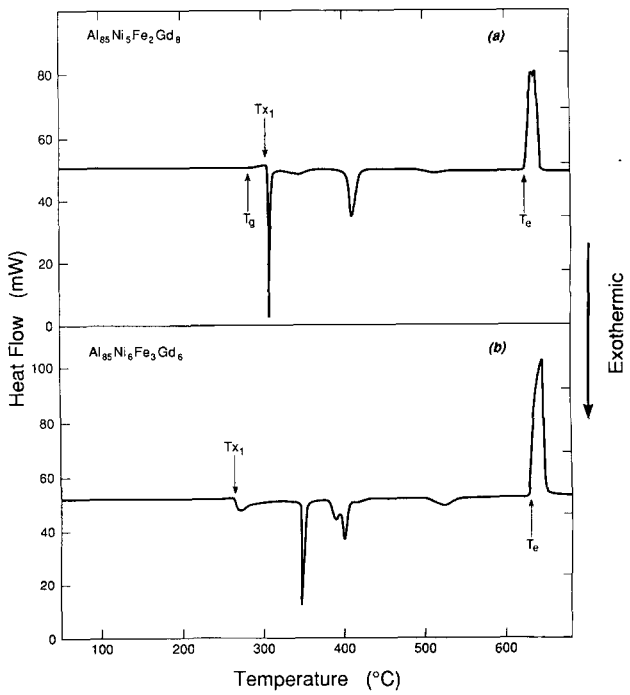

Fig. 3. DSC traces of (a) $Al_{85}Ni_5Fe_2Gd_8$ and (b) $Al_{85}Ni_6Fe_3Gd_6$ metallic glasses [10]. The temperature scanning rate is 20 K min^{-1}. Samples were obtained by melt-spinning at a wheel speed of 3600 rpm. While the first exothermic peak in $Al_{85}Ni_6Fe_3Gd_6$ corresponds to the primary crystallization of Al, no such peak is observed in $Al_{85}Ni_5Fe_2Gd_8$ amorphous ribbons.

TABLE 2. List of glass transition temperature (T_g), first crystallization temperature (T_x), eutectic melting temperature (T_m) and liquidus temperature (T_ℓ) of a few Al–TM–RE metallic glasses. The reduced glass temperature is $T_{rg}=T_g/T_\ell$. For some amorphous alloys, the crystallization takes place before glass transition, thus T_g cannot be observed.

Composition	T_g (K)	T_x (K)	T_m (K)	T_ℓ (K)	T_{rg}	Ref.
$Al_{85}Ni_5Fe_2Gd_8$	570	580	903	1283	0.44	10
$Al_{85}Ni_6Fe_3Gd_6$	–	529	903	1173	~0.49	10
$Al_{80}Fe_{10}Ce_{10}$	–	709	~925	1220	–	29
$Al_{80}Co_{10}Ce_{10}$	–	~711	~925	1065	–	29
$Al_{80}Fe_{10}Gd_{10}$	–	~740	~925	1420	–	29

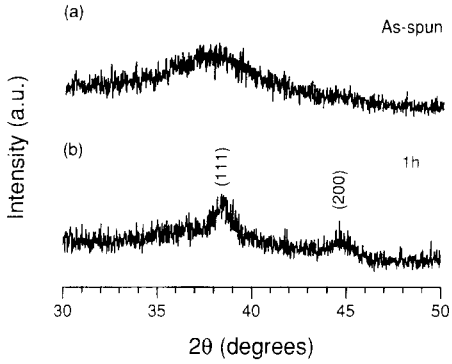

Fig. 4. X-Ray diffraction patterns of (a) as-spun $Al_{90}Fe_5Ce_5$ amorphous ribbons, (b) same ribbons after ball-milling for 1 h. Two crystalline peaks are visible, which can be indexed as (1 1 1) and (2 0 0) peaks of Al.

patterns [10]. $Al_{85}Ni_5Fe_2Gd_8$ became brittle after annealing while $Al_{85}Ni_6Fe_3Gd_6$ was still very flexible, although the annealing temperature is only about 50 °C lower than the first crystallization temperature in $Al_{85}Ni_6Fe_3Gd_6$. After annealing at 200 °C for 100 h, both samples were still amorphous without any detectable crystalline phases present. However, both samples became brittle after annealing. The embrittlement of metallic glasses after low temperature annealing has been previously noted [25]. For example, many Fe-based metallic glasses are ductile in the as-spun state but become brittle upon annealing as the result of structural relaxation [25]. A similar embrittlement mechanism maybe applicable to Al-based metallic glasses.

5.2. *Mechanical stability*

Thermally activated crystallization of amorphous alloys has been studied extensively. However, crystallization can also be induced by a mechanical driving force. Recently, we have observed the formation of nanocrystals within the shear bands of some Al-based metallic glasses induced by bending [26]. The observed crystallization is thought to be caused by the enormous plastic deformation inside the shear bands. Such mechanical deformation induced crystallization is also observed in the ball-milled amorphous alloys [16]. Figure 4(a) is an X-ray diffraction pattern of rapidly quenched $Al_{90}Fe_5Ce_5$ amorphous alloy. After ball-milling for 1 h, nanometer size Al crystals appear in the sample, as shown in Fig. 4(b). The mechanical stability of these Al-based amorphous alloys is not necessarily related to their thermal stability, and it is quite sensitive to the chemical composition of the alloy [16,26]. For example, no crystallization was observed upon ball-milling $Al_{85}Ni_5Y_{10}$ amorphous ribbons for 5 h, and DSC experiments showed that the crystallization peak shifted to higher temperatures after milling. The experimental details will be reported elsewhere.

6. Glass formability

There are many factors that can affect the glass-forming ability of an alloy. The atomic size mismatch, the heat of mixing, the short range order and the viscosity of the metal melts are a few of them. One of the most important factor influencing the glass formability of an alloy system is the reduced glass temperature T_{rg}, which is the ratio of the glass transition temperature T_g to the liquidus temperature T_l [25,27,28]. According to the conventional theory of metallic glass formation, the glass formation range usually coincides with a deep eutectic region in the phase diagram. Near the eutectic composition, the liquidus temperature of the alloy is lowered and the metallic liquid is stable to a lower temperature than in other regions of the phase diagram, so that it is easier to supercool the metal melt to below its glass temperature and bypass nucleation and crystallization [27,28]. Thus, T_{rg} can be used as a measure of glass formability of an alloy system. For good glass formers, conventional theory predicts $T_{rg}=0.65$–0.7 [28].

Quite different from the conventional glass-forming alloys, the liquidus temperatures of the aluminum alloys in study either increase or change little as the minority components are added to aluminum. DSC and differential thermal analysis (DTA) measurements revealed that upon alloying with transition metals and rare earths, the liquidus temperatures of these Al-alloys increase to around 900 °C or higher [10,29], which results in a reduced glass temperature of only 0.5 or less. However, these Al-alloys are found to be excellent glass-formers and can be quenched into amorphous states easily, even at low cooling rates [10]. In this sense, the glass formability of Al–TM–RE alloys is considered rather unique [7,10]. The glass transition temperature T_g, eutectic melting temperature T_m and the liquidus temperature T_l of several Al-based metallic glasses are listed in Table 2.

TABLE 3. Composition dependence of the lowest wheel speed required to make amorphous Al–Ni–Fe–Gd alloys [10] (x_c is the critical thickness)

Composition	Lowest wheel speed (rpm)	x_c (μm)
$Al_{85}Ni_5Fe_2Gd_8$	400	200
$Al_{85}Ni_6Fe_3Gd_6$	300	250
$Al_{85}Ni_7Fe_2Gd_6$	600	150–175
$Al_{87}Ni_6FeGd_6$	400	250
$Al_{83}Ni_6Fe_3Gd_8$	600[a]	150–175
$Al_{83}Ni_8Fe_2Gd_7$	600[a]	150–175
$Al_{83}Ni_{10}Fe_2Gd_5$	600[a]	150–175

[a]Mainly amorphous with some trace of crystalline phases when quenched at this speed.

It has been found that the addition of a second transition metal in Al–TM–RE alloys allow improvement of glass formability and mechanical properties [9,10]. For example, adding Ni to Al–Fe–Gd alloys dramatically increases the glass formability and the tensile strength [10]. The minimum wheel speed required for glass formation and the corresponding maximum ribbon thickness of several Al–Ni–Fe–Gd alloys are given in Table 3. From this table it can be concluded that despite the low reduced glass temperature observed in these Al-alloys, sub-millimeter thick amorphous ribbons can be produced at relatively low cooling rates, suggesting that the glass forming ability of these Al-alloys is very good.

7. Conclusions

New Al–TM–RE amorphous alloys with high mechanical strength and low density have been produced by a melt-spinning method. For some of these alloys, the tensile strength σ_f approaches $E/50$, the theoretical value. Thermal analysis revealed that the formation of these Al-based amorphous alloys is rather unusual. Sub-millimeter thick amorphous ribbons can be produced at low cooling rates. Structural studies revealed that the Al–TM bond in these amorphous alloys is anomalously short, indicating a strong interaction between Al and transition metal atoms, which may be the cause of the good glass formability and high mechanical strength of these amorphous alloys. Rare earth atoms, which are distributed randomly in the amorphous alloy, play an important role in stabilizing the liquid-like structure. High tensile strengths combined with good glass formability make these Al glasses ideal candidates for high-strength low-density materials.

Acknowledgment

Financial support from US Army Research Office through contract No. DAAL-03-91-G-0009 is acknowledged.

References

1 W. Klement, R.H. Willens and P. Duwez, *Nature, 187* (1960) 869.
2 See, for example, F.E. Luborsky (ed.), *Amorphous Metallic Alloys*, Butterworths, Boston, 1983.
3 S. Takayama, *J. Mater. Sci., 11* (1976) 164.
4 R.W. Cahn, *Nature, 341* (1989) 183.
5 A. Inoue, A. Kitamura and T. Masumoto, *J. Mater. Sci., 16* (1981) 1895.
6 R.O. Suzuki, Y. Komatsu, K.E. Kobayashi and P.H. Shingu, *J. Mater. Sci., 18* (1983) 1195.
7 Y. He, S.J. Poon and G.J. Shiflet, *Science, 241* (1988) 1640.
8 A. Inoue, K. Ohtera, A.P. Tsai and T. Masumoto, *Jpn. J. Appl. Phys., 27* (1988) L479.
9 A. Inoue, N. Matsumoto and T. Masumoto, *Mater. Trans. JIM, 31* (1990) 493.
10 Y. He, G.M. Dougherty, G.J. Shiflet and S.J. Poon, *Acta Metall. Mater., 41* (1993) 337.
11 S. Samson, *Acta Crystallogr., 11* (1958) 851.
12 A. Inoue, K. Ohtera, K. Kita and T. Masumoto, *Jpn. J. Appl. Phys., 27* (1988) L1796.
13 C. Price, Y. He, S.J. Poon and G.J. Shiflet, unpublished results, University of Virginia, 1993.
14 A. Inoue, K. Ohtera and T. Masumoto, *Jpn. J. Appl. Phys., 27* (1988) L736.
15 A. Inoue, K. Ohtera, T. Zhang and T. Masumoto, *Jpn. J. Appl. Phys., 27* (1988) L1583.
16 Y. He, G.J. Shiflet and S.J. Poon, *Acta Metall. Mater.*, accepted for publication.
17 G.J. Shiflet, Y. He and S.J. Poon, *Scripta Metall., 22* (1988) 1661.
18 F. Spaepen and A.I. Taub, in F.E. Luborsky (ed.), *Amorphous Metallic Alloys*, Butterworths, Boston, 1983, p. 231.
19 Y. He, H. Chen, G.J. Shiflet and S.J. Poon, *Philos. Mag. Lett., 61* (1990) 297.
20 L.C. Chen and F. Spaepen, *Nature, 336* (1988) 366.
21 H.Y. Hsieh, B.H. Toby, T. Egami, Y. He, S.J. Poon and G.J. Shiflet, *J. Mater. Res., 5* (1990) 2807.
22 H.Y. Hsieh, T. Egami, Y. He, S.J. Poon and G.J. Shiflet, *J. Non-Cryst. Solids, 135* (1991) 248.
23 T. Egami, *Mater. Trans. JIM, 31* (1990) 163.
24 H.S. Chen and D. Turnbull, *Appl. Phys. Lett., 10* (1967) 284.
25 See, for example: H.S. Chen, *Rep. Prog. Phys., 43* (1980) 23.
26 H. Chen, Y. He, G.J. Shiflet and S.J. Poon, *Nature, 367* (1994) 541.
27 F. Spaepen and D. Turnbull, *Annu. Rev. Phys. Chem., 35* (1984) 241.
28 H.A. Davies, in F.E. Luborsky (ed.), *Amorphous Metallic Alloys*, Butterworths, Boston, 1983, p. 8.
29 L.T. Kabacoff, C.P. Wong, N.L. Guthrie and S. Dallek, *Mater. Sci. Eng., A134* (1991) 1288.